AD-A078 845 SRI INTERNATIONAL MENLO PARK CA F/G 21/9.2
DEFLAGRATION-TO-DETONATION TRANSITION IN HMX-BASED PROPELLANTS.(U)
AUG 79 M COMPERTHWAITE , W J MURRI F49620-77-C-0039
UNCLASSIFIED AFOSR-TR-79-1286 NL

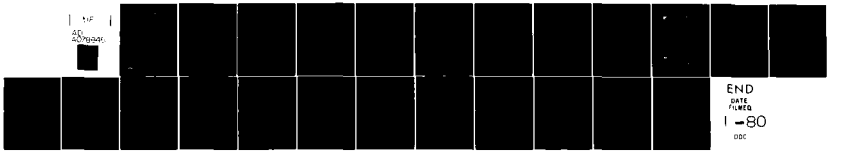

END
DATE FILMED
1-80
DDC

AFOSR-TR-79-1286

LEVEL II

Aug 1979

Interim Report
Covering the period 1 May 1978 to 30 April 1979

DEFLAGRATION-TO-DETONATION TRANSITION IN HMX-BASED PROPELLANTS

By: M. Cowperthwaite, W. J. Murri and J. T. Rosenberg

Prepared for:

AIR FORCE OFFICE OF SCIENTIFIC RESEARCH
Aerospace Sciences Directorate
Bldg. 410
Bolling Air Force Base
Washington, D.C. 20322

Contract F49620-77-C-0039

SRI Project PYU-6069

Approved by:

79 12 18 10

G. R. Abrahamson, Director
Poulter Laboratory
Physical Sciences Division

Approved for public release;
distribution unlimited.

SRI International
333 Ravenswood Ave. • Menlo Park, California 94025
(415) 326-6200 • Cable: SRI INTL MPK • TWX: 910-373-1246

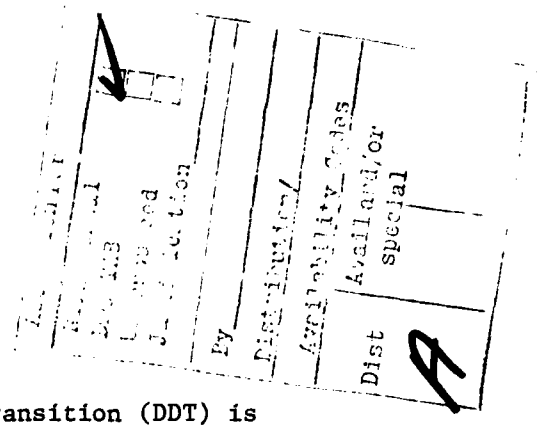

I INTRODUCTION

Research on the deflagration-to-detonation transition (DDT) is important to the Air Force because many of the energetic propellants required for present and future long-range delivery systems are explosively-filled compositions that are capable for undergoing DDT. HMX-based propellant, for example, usually burns reliably in rocket motors. On several occasions, however, it has detonated and destroyed the motors. Possible causes that lead to detonation in a rocket motor are fracture of propellant ahead of the flame and the subsequent formation of shock waves produced by the increased burning rate of fractured propellant. But even in this case, the mechanism of DDT and the conditions for its initiation are not adequately understood.

The long-range objective of the present research program is to develop a computational capability for assessing the DDT hazard in explosively-filled propellants. The program is based on the concept that an understanding of the fundamental physical and chemical processes involved in one-dimensional DDT is necessary if the objective is to be achieved. Combined theoretical and experimental studies to determine the pressure fields behind and ahead of the flame and to establish the mechanisms of DDT are required.

II THEORETICAL STUDIES

In the theoretical study, attention was given to the factors governing shock formation in front of an accelerating flame. Formation of a shock is necessary for the onset of DDT because detonation is a shock that is supported by a chemical reaction. The flame was treated simply as a reactive discontinuity.

Let t denote time, h the Lagrange distance, v the specific volume, u the particle velocity, σ the stress, and e the specific energy. The subscript o will denote the compressed material in front of the flame and the subscript f will denote quantities associated with the flame. The one-dimensional flow in front of the flame is governed by the following differential equations

$$\left(\frac{\partial v}{\partial t}\right)_h = v_o \left(\frac{\partial u}{\partial h}\right)_t \quad , \tag{1}$$

$$\left(\frac{\partial u}{\partial t}\right)_h = - v_o \left(\frac{\partial \sigma}{\partial h}\right)_t \quad , \tag{2}$$

and

$$\left(\frac{\partial e}{\partial t}\right)_h = - \sigma \left(\frac{\partial v}{\partial t}\right)_h \quad , \tag{3}$$

which express the conservation of mass, momentum, and energy, respectively. The flame is governed by the Rankine-Hugoniot jump conditions

$$v_-(F - u_+) = v_+(F - u_-) \quad , \tag{4}$$

$$(u_- - u_+)^2 = (p_- - p_+)(v_+ - v_-) \quad , \tag{5}$$

and

$$2(e_- - e_+) = (p_- + p_+)(v_+ - v_-) \quad , \tag{6}$$

where F denotes the Eulerian velocity of the flame and the subscripts + and - denote the initial and final states, respectively, connected by the flame.

It is convenient in considering shock formation to rewrite Eqs. (1) and (2) as

$$- v_o \left(\frac{\partial u}{\partial v}\right)_h = \left(\frac{\partial h}{\partial t}\right)_u = C_u \tag{7}$$

and

$$v_o \left(\frac{\partial \sigma}{\partial u}\right)_h = \left(\frac{\partial h}{\partial t}\right)_\sigma = C_\sigma \quad . \tag{8}$$

Equations (7) and (8) are also useful for purposes of the Lagrange analysis. The quantities C_u and C_σ are, respectively, the slopes of the curves of constant particle velocity and stress in the (t,h) plane. In other words, the points of constant particle velocity in a wave propagate at C_u and the points of constant stress propagate at C_σ. A shock will be formed in the compressive part of a wave when the wave profile steepens as the wave propagates. The conditions for compressive wave steepening, $(\partial C_u/\partial u)_h > 0$ and $(\partial C_\sigma/\partial \sigma)_h > 0$, are thus kinematic conditions for shock formation. These conditions are related to dynamic material properties by the following equations

$$\left(\frac{\partial C_u}{\partial u}\right)_h = - v_o \frac{(\partial^2 u/\partial v^2)_h}{(\partial u/\partial v)_h} \tag{9}$$

and

$$\left(\frac{\partial C_\sigma}{\partial \sigma}\right)_h = v_o \frac{(\partial^2 \sigma/\partial u^2)_h}{(\partial \sigma/\partial u)_h} \quad , \tag{10}$$

obtained by differentiating Eq. (7) partially with respect to u and differentiating Eq. (8) partially with respect to σ. Because $(\partial u/\partial v)_h < 0$ and $(\partial \sigma/\partial u_h > 0$ during compression, the dynamic material properties associated with shock formation follow readily from Eq. (9) and Eq. (10) as $(\partial^2 u/\partial v^2)_h > 0$ and $(\partial^2 \sigma/\partial u^2)_h > 0$.

Properties of the Lagrange stress-strain curve associated with shock formation are obtained from the equation

$$\left(\frac{\partial\sigma}{\partial v}\right)_h = -\frac{C_\sigma C_u}{v_o^2} \quad , \tag{11}$$

obtained by combining Eqs. (7) and (8). Differentiation of Eq. (11) gives the equation

$$-v_o^2 \frac{(\partial^2\sigma/\partial v^2)_h}{(\partial\sigma/\partial v)_h} = v_o(\partial C_u/\partial u)_h + C_u(\partial C_\sigma/\partial\sigma)_h \quad ; \tag{12}$$

the condition that the Lagrange (σ,v) relationship must satisfy for shock formation to occur in compression follows as $(\partial^2\sigma/\partial v^2)_h > 0$ because $(\partial\sigma/\partial v)_h < 0$.

We will now consider shock formation in a simple wave adjacent to a constant state. In a simple wave, the stress and specific volume are functions only of particle velocity.* $C_\sigma = C_u$, and the curves of constant particle velocity, of constant stress, and of constant volume are straight lines. Equation (11) can then be written as

$$\left(\frac{\partial\sigma}{\partial v}\right)_h = -\left(\frac{C_\sigma}{v_o}\right)^2 = -\left(\frac{C_u}{v_o}\right)^2 , \tag{13}$$

and differentrated to give the equations

$$-\frac{v_o}{2}\frac{(\partial^2\sigma/\partial v^2)_h}{(\partial\sigma/\partial v)_h} = \frac{C_\sigma}{v_o}\left(\frac{\partial C_\sigma}{\partial\sigma}\right)_h = \left(\frac{\partial C_u}{\partial u}\right)_h \quad . \tag{14}$$

*M. Cowperthwaite and R. F. Williams, "Determination of Constitutive Relations with Multiple Gages in Nondivergent Waves," J. Appl. Phys, 42, (1971), p. 456.

These equations again show that the condition $(\partial^2\sigma/\partial v^2)_h > 0$ must be satisfied for shock formation. In classical work, simple waves are treated in terms of characteristic curves. The differential equation for the characteristic curves is

$$\frac{dh}{dt} = \pm \frac{v_o c}{v} \tag{15}$$

where the sound speed c is defined by the identity $(c/v)^2 = -(\partial p/\partial v)_s$ and where s denotes entropy and p denotes pressure. The characteristics associated with the plus sign are called C_+ characteristics and those associated with the minus sign are called C_- characteristics. At this stage we identify the stress with the pressure, set $\sigma = p$ accordingly, and use the $e = e(s,v)$ equation of state to rewrite Eq. (3) as

$$\left(\frac{\partial s}{\partial t}\right)_h = 0 \quad . \tag{16}$$

It then follows from Eq. (11), Eq. (16), and the identity

$$\left(\frac{\partial p}{\partial v}\right)_h = \left(\frac{\partial p}{\partial v}\right)_s + \left(\frac{\partial p}{\partial s}\right)_v \left(\frac{\partial s}{\partial t}\right)_h \quad , \tag{17}$$

that

$$-\left(\frac{\partial p}{\partial v}\right)_h = \frac{C_p C_u}{v_o^2} = \frac{c^2}{v^2} \tag{18}$$

Equation (14) for the simple wave can then be written as

$$\frac{dh}{dt} = \pm C_u \tag{19}$$

and it follows that the characteristics coincide with the curves of constant particle velocity and are straight lines.

We will now consider shock formation in a simple wave produced by an accelerating piston or an accelerating flame. A shock is formed where the forward facing characteristics emanating from the piston or the flame intersect to form an envelope. Integrating Eq. (19) gives the particle velocity field for the flow produced by a piston as

$$h = C_u[t - t_p(u)] \quad , \tag{20}$$

where the subscript P denotes the piston, and gives the particle velocity field for the flow produced by the flame as

$$h = h_f(u) + C_u(t - t_f(u)) \quad . \tag{21}$$

The condition that the derivative $(\partial h/\partial u)_t$ vanishes on the envelope formed by the characteristics gives the parametric representation of this envelope as

$$t_e = t_p(u) + \frac{C_u}{(du_p/dt)(dC_u/du)} \tag{22}$$

and

$$h_e = \frac{C_u^2}{(du_p/dt)(dC_u/du)} \quad , \tag{23}$$

where $(dC_u/du) = -v_o(\partial^2 p/\partial v^2)_s/2(\partial p/\partial v)_s$. Equations (22) and (23) show that the C_+ characteristics emanating from an accelerating piston $du_p/dt > 0$ form an envelope in front of the piston $h_p = 0$ when $(\partial^2 p/\partial v^2)_s > 0$. Let the subscript i denote the initial condition at the origin. When $(du_p/dt)_i > 0$, the shock is formed at the point $t = t_c$, $h = c_o t_c$ on the C_+ characteristic through the origin; t_c is given by Eq. (22) as

$$t_c = \frac{c_o}{(du_p/dt)_i (dC_u/du)_i} \quad . \tag{24}$$

The parametric representation of the envelope associated with an accelerating flame is obtained from Eq. (21) as

$$t_e = t_f(u) + \frac{(C_u - dh_f/dt)}{(du_f/dt)(dC_u/du)} \tag{25}$$

and

$$h_e = h_f(u) + C_u \frac{(C_u - dh_f/dt)}{(du_f/dt)(dC_u/du)} \quad . \tag{26}$$

We consider a flame with an initial velocity $(dh_f/dt)_i = 0$ but with an initial acceleration $(du_f/dt)_i > 0$. In this case, as with the accelerating piston, the shock is formed at the point $t = t_c$, $h = c_o t_c$ on the C_+ characteristic through the origin; the time t_c is given by

$$t_c = \frac{c_o}{(du_f/dt)_i (dC_u/du)_i} \tag{27}$$

from Eq. (25).

It is clear, in contrast to the case of the accelerating piston, that there is a class of accelerating flames that is associated with shock formation and a class that is not. These classes are separated by the accelerating flame that overtakes the first characteristic at the time t_c. A shock is formed by accelerating flames that would overtake the first characteristic after t_c but not by accelerating flames that overtake the first characteristic before t_c. Solutions for such flows will be considered in future work.

III EXPERIMENTAL STUDIES

The purpose of the experiments described in this section was to obtain stress-time measurements in a propellant as it underwent the transition from one-dimensional deflagration to detonation. Additionally, we hoped to measure the flame velocity in the propellant. The experimental arrangement, shown in Figure 1, consisted of a thick-walled steel confinement tube, end plugs, an igniter cup, a PMMA tube containing the propellant and stress gages, and bolts and nuts to clamp the end plugs tightly to the confinement tube.

DDT Confinement Tube

The confinement tube was made of 4142 steel. It was 28 in. long with an inside diameter of 3 in. and an outside diameter of 7 in. The confinement tube, end plugs, and clamping bolts were designed to confine the high gas pressures generated in the igniter region and by the burning propellant until pressures of the order of thousands of bars were reached. The inside diameter of the tube was large enough to make any diameter effect on burning negligible and to exceed the critical diameter of the propellant. The end plug at the igniter end had a hole through which the igniter leads were passed.

Igniter

The igniter material was a mixture of boron and potassium nitrate with a laminac-lubersol binder obtained from Polytechnic Specialties in Byron, Georgia. The mixture was 22.7% boron, 71.7% potassium nitrate, and 5.6% binder. This mixture generates about 1600 cal/g of material. About 10 g of the igniter powder was placed in a Lucite cup lined on the bottom with a nichrome heating ribbon. The cup had an inside diameter of 2.5 in. and a depth of 0.25 in. The nichrome ribbon was about 11 in. long, 0.06 in. wide, and 0.007 in. thick; it had a resistance of about 1 ohm.

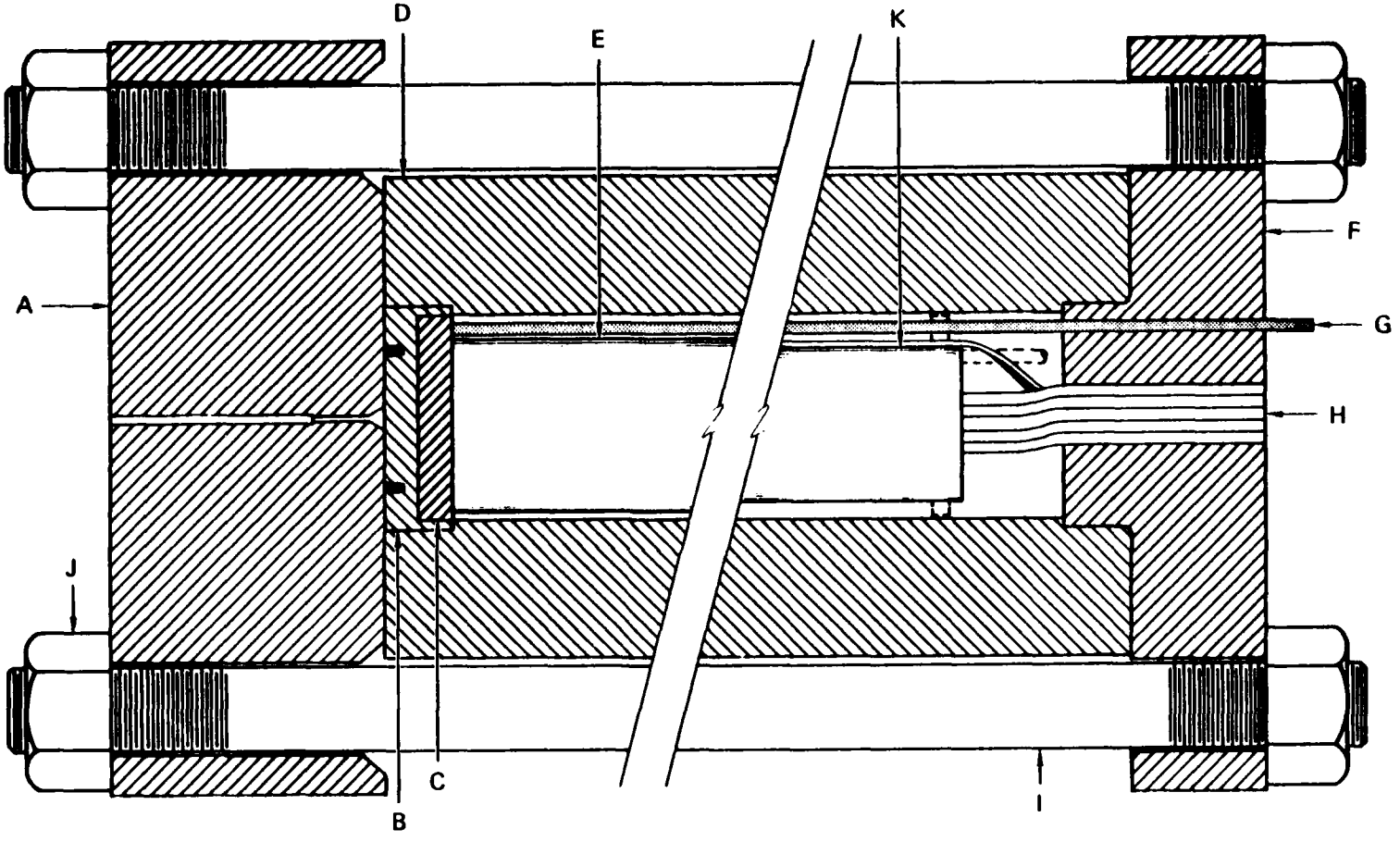

FIGURE 1 SCHEMATIC DRAWING OF EXPERIMENTAL ARRANGEMENT

A – Igniter end plug; B – Igniter cup holder; C – Igniter; D – steel DDT confinement cylinder; E – tube containing propellant; F – End plug; G – Light pipe; H – Leads from stress gages and ionization pins; I – High strength bolts; J – Nuts; K – Backing tube containing gage leads and epoxy. All regions within the DDT tube shown as voids are filled with epoxy.

The igniter material was thermally initiated using a 28 V, 5 A., dc power supply to actuate the nichrome heating ribbon.

Propellant Tube and Propellant

The Lucite tube used to contain the propellant inside the steel DDT tube is shown in Figure 2 as it appears before the propellant is poured into it. The purpose of this tube is to serve as a casting mold for the propellant and as a jig for holding the gages during casting. The main section of the Lucite tube is 10 in. long and has an inside diameter of 2 in. This section was slit lengthwise down the center of the cylinder for the purpose of supporting the gages. Three ytterbium stress gages were glued to a sheet of Kapton,* their leads insulated from one another by additional pieces of Kapton. The resulting Kapton sheet with gages was then glued between the two Lucite half cylinders, as shown in Figure 2. The stress gages were located 1, 2, and 3 in. from the end of the cylinder. The gage leads were attached to Twinax† coaxial cable and potted with epoxy inside a Lucite backing tube that had an outside diameter of 2.25 in. (Fig. 2). The purpose of the backing tube was to delay the arrival at the measuring stations of stress waves reflected from the end of the DDT tube. The entire assembly, propellant and backing tube, was 22.375 in. long. Three ionization pins were placed in the tube at points that were 0.25, 0.5, and 0.75 in. from the end.

After the stress gages and ionization pins were emplaced, the tubes were sent to Edwards Air Force Base, where the propellant was cast in them. Our original plan was to use propellant containing approximately 50% HMX. However, because of the propellant classification regulations in force at the time, the propellant we obtained contained approximately 12% HMX. A number of 1-in-long sections of Lucite tube of the same diameter as the propellant tube were also sent to Edwards Air Force Base.

*Kapton is a registered trademark of Du Pont for polyimide film.

†Twinax is a two-conductor-shielded coaxial cable manufactured by Trompeter Electronics.

These 1-in. sections, termed add-on sections, were filled with either solid or powdered propellant. The powdered propellant supplied for the experiments exhibited a rate of pressure rise of 2.5×10^6 psi/sec in a quickness test performed by personnel at Edwards Air Force Base. Each of the 1-in. add-on sections contained four ionization pins. The pins, 0.25-in. apart, were used to measure the burning rate in the propellant. The purpose of the add-on sections is described in the next section.

Experimental Arrangement

Two 1-in-long add-on sections were added in front of the 10-in. main section of solid propellant in each experiment. By using various combinations of powered and solid filled add-on sections, we could control the burning rate in the propellant and observe the effect on stress wave propagation and buildup at the stress gages in the main section ahead of the flame front. Three experiments were conducted; the following table gives the arrangement of the propellant add-on sections. The 10-in. main section, in which the stress gages were emplaced, was used in all experiments.

Table 1

ARRANGEMENT OF PROPELLANT SECTIONS

	Experiment Number		
Propellant Section	1	2	3
First Add-on Section	Solid[a]	Powdered[b]	Powdered[b]
Second Add-on Section	Powdered[b]	Powdered[b]	Solid[a]

[a]Density = 1.95 g/cm^3.

[b]Density = 1.51 g/cm^3.

The add-on sections were taped to the 10-in solid-propellant section, and a light pipe was epoxied to the outside of the combined cylinder so as to be flush with the igniter end of the propellant tube. The entire propellant tube--containing stress gages, ionization pins, and light pipe--was then placed inside the steel DDT tube so as to butt against the igniter (see Fig. 1). After alignment, the cavity between the propellant tube and the inside diameter of the steel DDT cylinder was filled with epoxy. We used stycast low viscosity Resin No. 3020 with catalyst No. 9.* Because this epoxy has a low exotherm temperature (∿30°C) it was safe to use with the propellant. A dummy igniter was used to hold the components in the proper positions during the epoxy pour. After the epoxy had hardened, the dummy igniter was removed and the real igniter was inserted and the end caps bolted together. The bolts, 1.25 in. in diameter, were torqued to 1,000 ft-lb each. The leads for the stress gages and ionization pins exited through the end cap opposite the igniter as shown in Figure 1. The space around the leads was filled with epoxy.

Instrumentation

The signals from the stress gages and ionization pins were recorded on oscilloscopes. The signal from the light pipe, produced when the burning in the igniter mixture reached the igniter-propellant interface, was used to trigger the oscilloscopes; the oscilloscopes recorded the stress gage signals. The power supplies for the stress gages were turned on by the "gate out" from the oscilloscopes recording the stress gage signals. The oscilloscopes used to record the ionization pins were internally triggered by the signal coming from the first pin to close. One oscilloscope, triggered by the signal from the light pipe, recorded the signal from the pins. The record from this latter oscilloscope was used to time-correlate the stress gages and the ionization pins.

*From Emerson and Cummings, Inc., Gardena, Calif. 90248.

Experimental Results and Interpretation

Table 1 shows the arrangement of cracked and solid propellant in the three experiments that were performed. The results of each experiment will be discussed and then some general conclusions will be given.

In the first experiment, in which we had expected stresses of the order of 40 kbars, the stress gages recorded stresses of only about 5 to 7 kbar. Such low stresses indicate that the burning did not produce high-order detonation. Because the instrumentation was set for the expected high stresses, the stress gage records obtained were not of optium quality. No pin records were obtained from this experiment.

Examination of the recovered hardware indicates that at some point during the experiment, venting occurred between the steel DDT cylinder and the end cap at the igniter end. The hardware was recovered still completely assembled but the bolts had stretched under the internal pressure generated by the burning igniter and propellant. After the experiment, there was a 0.125-in. gap between the igniter end cap and the DDT cylinder. Markings on the hardware indicate that the igniter cup was forced backward and that the hot gasses escaped between the igniter cup and the DDT cylinder. These escaping gases eroded the surfaces of the cup and the inside of the DDT cylinder. Figure 3 shows the loose fit between the igniter cup and the steel cylinder; the pre-shot tolerance of this fit was 0.003 in. Figures 4(a) and (b) show that the hot escaping gases also eroded the end cap and the bolts.

Although stronger bolts were used in the second and third experiments, venting still occurred and the recovered hardware looked the same as that in the first experiment. The hot escaping gases eroded parts of the end cap, the bolts, and the igniter cup. Interestingly, we recovered pieces of Lucite from inside the confinement cylinder that did not look like they had been melted.

Stress gage records were obtained from all gages in the second and third experiments. Figure 5 shows the oscilloscope records from Experiment No. 3 and Figure 6 shows the corresponding reduced stress-time profiles. The data in Figures 5 and 6 indicate a steady state of stress

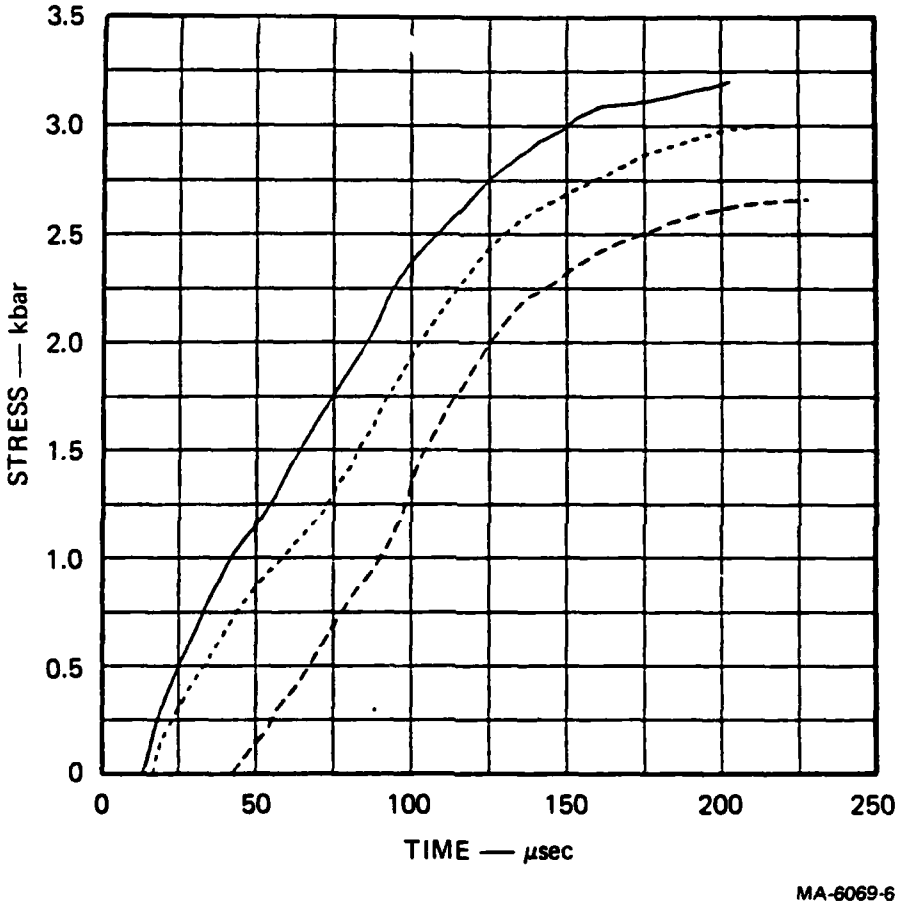

FIGURE 6 STRESS HISTORIES IN PROPELLANT OBTAINED FROM GAGE RECORDS OF EXPERIMENT 3 AND USED FOR LAGRANGE ANALYSIS

at each gage position about 100 to 200 μsec after the initial rise. The steady state of stress decreases from gages 1 to 3, however, indicating that the propellant maintains a stress gradient. Gage 3 from experiment 3 recorded for the longest time--about 900 μsec.

The stress waves arrive at the gages much sooner than the flame front. In the first experiment, the stress waves arrived at gage 3 (the best record) about 480 μsec after the flame reached the igniter-propellant interface. In the second and third experiments, the stress waves arrived at the gages just at the time the flame reached the igniter-propellant interface. Two reasons for this difference are suggested. In the first experiment, weaker bolts were used and the venting may have occurred early causing a slower pressure buildup. Also, in the first experiment the first propellant add on section after the igniter was solid propellant, whereas in the second and third experiments the first add on propellant section was powdered propellant. Thus, the gas generated by the igniter might have entered the propellant more readily in the latter two experiments, resulting in the earlier generation of stress waves.

Good quality ionization pin records were obtained for experiment No. 3. Seven pin signals were recorded; the results are shown on a distance-time plot in Figure 7. There is a decided change in slope in the pin results at about 900 μsec. The burning rate determined from the pin data (ignoring the first pin) up to that point was 0.068 mm/μsec. After about 900 μsec, the burning rate slowed to about 0.021 mm/μsec.

Lagrange Analysis

The Lagrange stress histories shown in Figure 6 based on the experimental data, were used in a Lagrange analysis to calculate Lagrange particle velocity histories, Lagrange stress-particle velocity paths, and Lagrange stress-specific volume paths in compressed propellant ahead of the frame front. In the Lagrange analysis, the momentum equation is integrated with the stress gradient estimated from the stress records to generate the particle velocity histories at the gage positions.

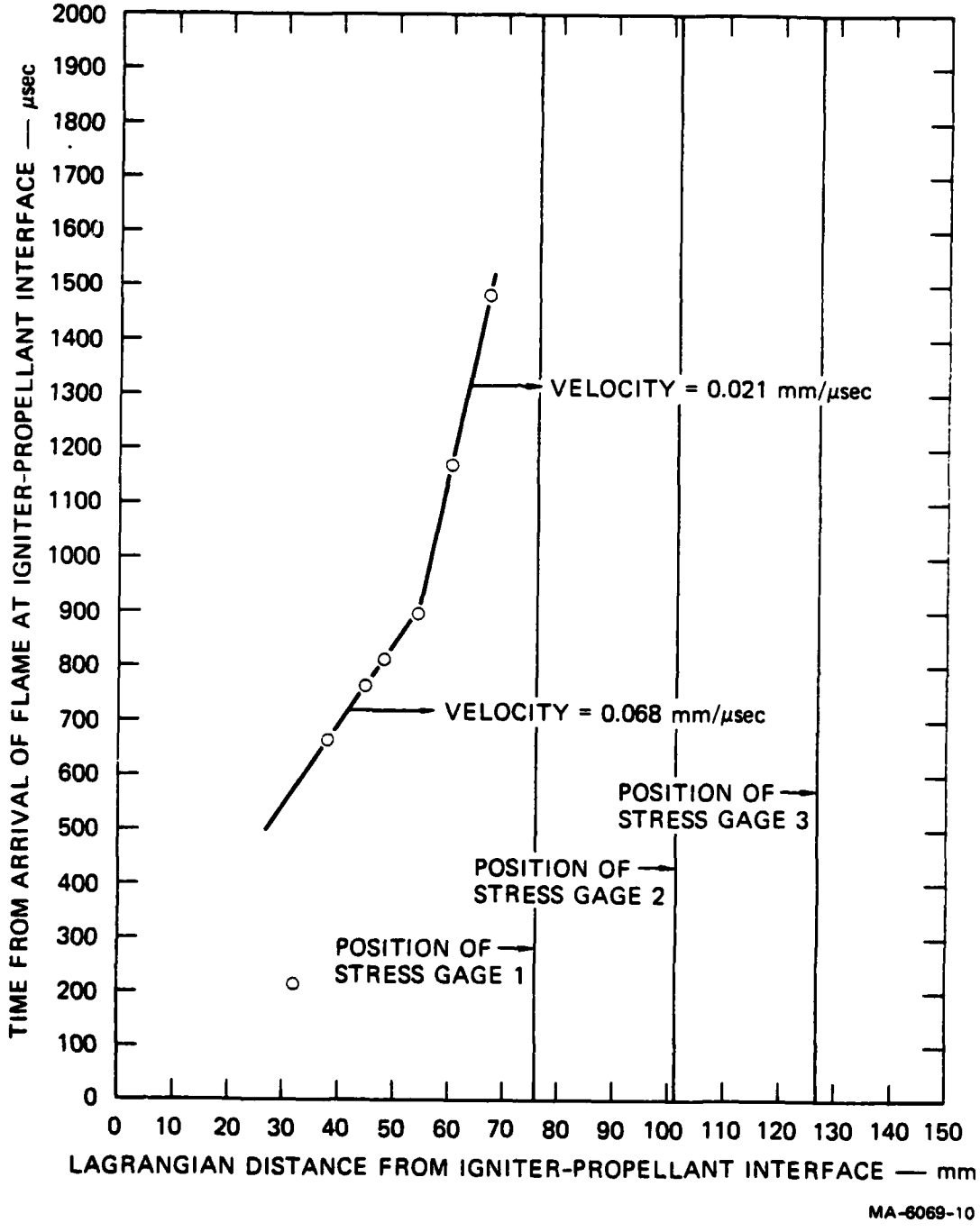

FIGURE 7 IONIZATION PIN DATA

The continuity equation is then integrated with the particle velocity gradient estimated from the particle velocity histories to generate the specific volume histories at the gage positions. The elimination of time between the stress histories and the particle velocity histories gives the corresponding Lagrange stress-specific volume paths. The (u,t) profiles calculated from the (σ,t) records are shown in Figure 8, and the corresponding Lagrange (σ,u) paths and Lagrange (σ,v) paths are shown in Figures 9 and 10.

Examination of these profiles shows that the flame produces a compression wave ahead of itself as it propagates along the tube. The stress at a given gage position builds up to a constant value and a constant Lagrange pressure gradient is formed in the compression ahead of the flame. A shock is not formed in front of the flame because as shown in Figures 9 and 10 the propellant satisfies the conditions $(\partial^2\sigma/\partial u^2)_h < 0$ and $(\partial^2\sigma/\partial v^2)_h < 0$ in the pressure range produced by the flame. The limited buildup in pressure is attributed to the relatively small amount of HMX in the propellant. Shock formation is expected at higher pressures in this propellant, however, because these second derivatives become positive as the pressure increases. DDT experiments with propellant containing more than 50% HMX will be performed in the next experimental study.

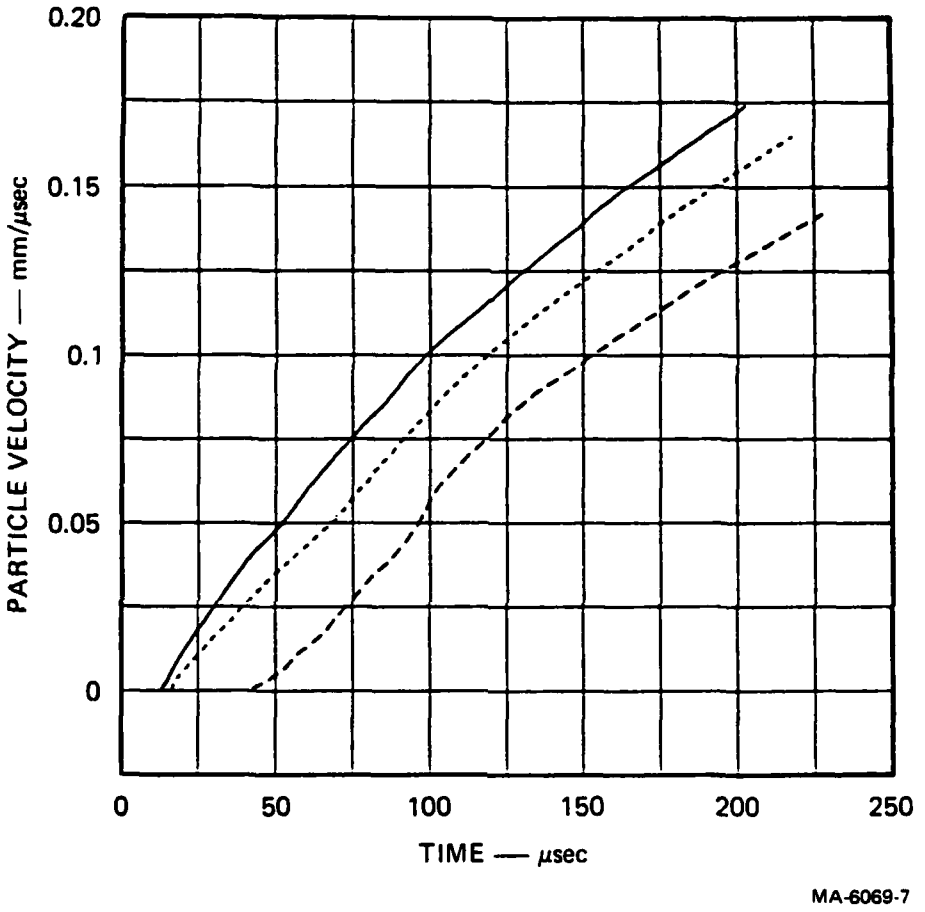

FIGURE 8 PARTICLE VELOCITY HISTORIES CALCULATED FROM THE STRESS HISTORIES SHOWN IN FIGURE 6

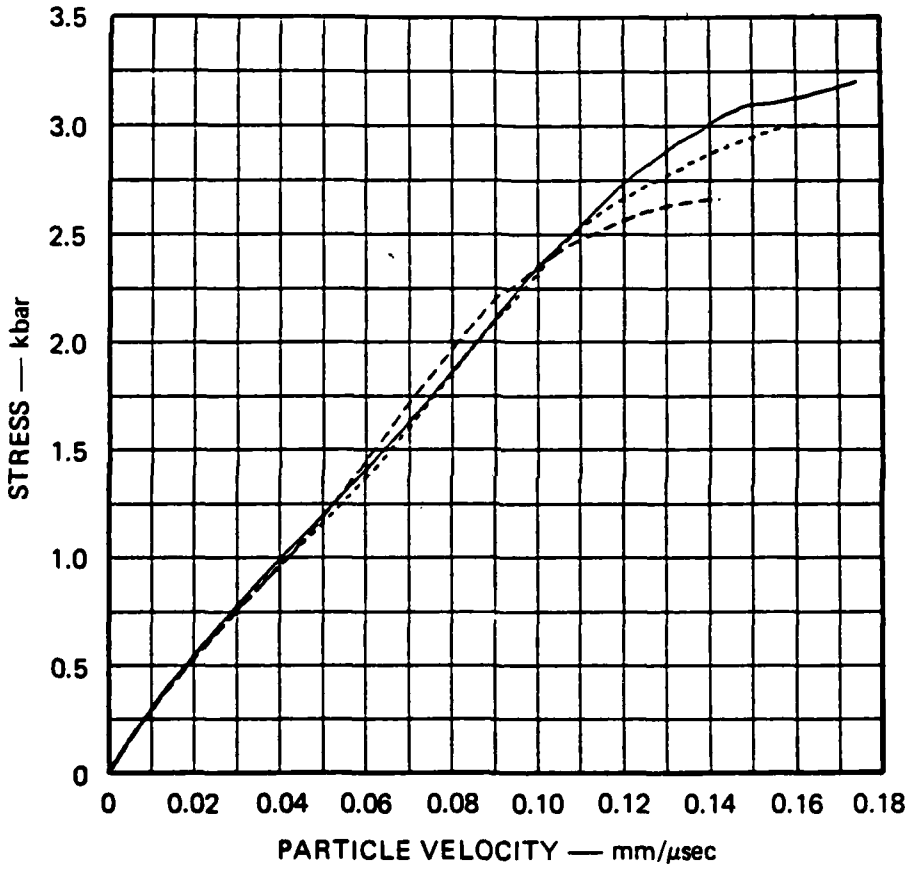

FIGURE 9 LAGRANGE STRESS-PARTICLE VELOCITY PATHS CALCULATED FROM THE STRESS HISTORIES SHOWN IN FIGURE 6

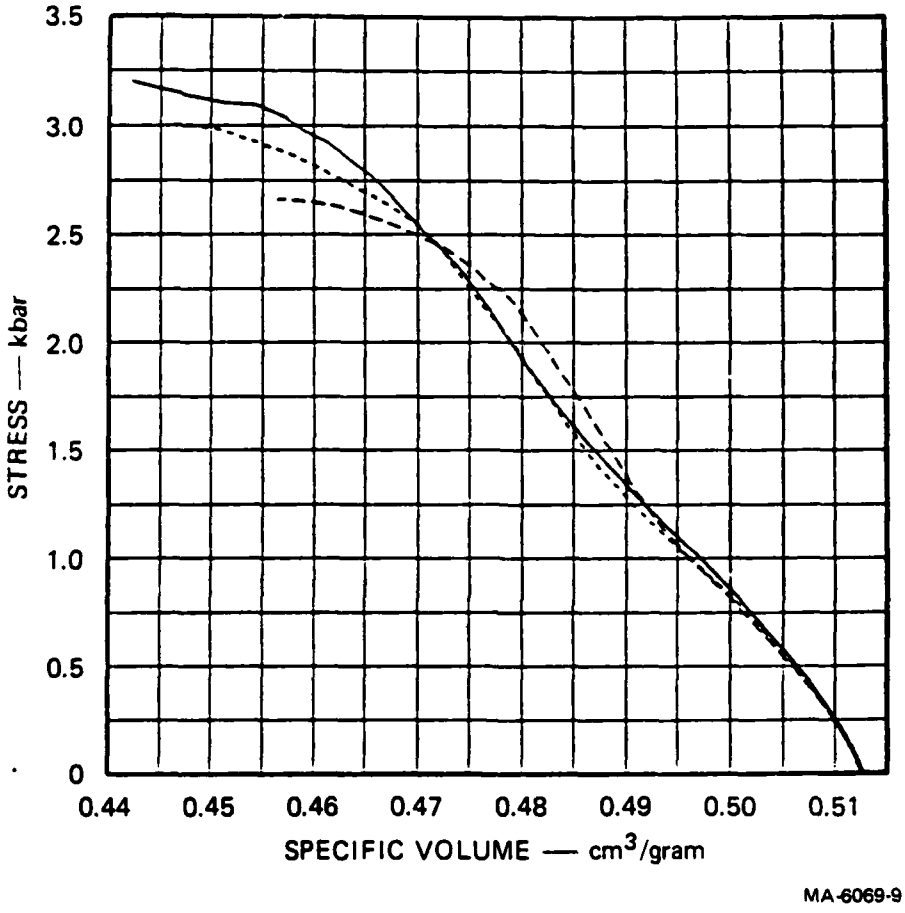

FIGURE 10 LAGRANGE STRESS-VOLUME PATHS CALCULATED FROM THE STRESS HISTORIES SHOWN IN FIGURE 6

IV FUTURE WORK

Solutions for the flow produced by an accelerating flame will be constructed and a series of Lagrange gage DDT experiments will be performed with propellant containing more than 50% HMX, since Edwards Air Force Base is now able to ship us propellant containing more than 50% HMX. We expect that the greater HMX content will permit the expensive and complex confinement procedures used in the present program to be simplified and still allow us to observe DDT.

SECURITY CLASSIFICATION OF THIS PAGE (When Data Entered) Unclassified

REPORT DOCUMENTATION PAGE	READ INSTRUCTIONS BEFORE COMPLETING FORM
1. REPORT NUMBER AFOSR-TR- 79-1286 / 2. GOVT ACCESSION NO.	3. RECIPIENT'S CATALOG NUMBER
4. TITLE (and Subtitle) DEFLAGRATION-TO-DETONATION TRANSITION IN HMX-BASED PROPELLANTS	5. TYPE OF REPORT & PERIOD COVERED INTERIM 1 May 78 - 30 Apr 79
	6. PERFORMING ORG. REPORT NUMBER PYU-6069
7. AUTHOR(s) M COWPERTHWAITE W J MURRI J T ROSENBERG	8. CONTRACT OR GRANT NUMBER(s) F49620-77-C-0039
9. PERFORMING ORGANIZATION NAME AND ADDRESS SRI INTERNATIONAL 333 RAVENSWOOD AVENUE MENLO PARK, CA 94025	10. PROGRAM ELEMENT, PROJECT, TASK AREA & WORK UNIT NUMBERS 2308A1 61102F
11. CONTROLLING OFFICE NAME AND ADDRESS AIR FORCE OFFICE OF SCIENTIFIC RESEARCH/NA BLDG 410 BOLLING AIR FORCE BASE, D C 20332	12. REPORT DATE Aug 79
	13. NUMBER OF PAGES 26
14. MONITORING AGENCY NAME & ADDRESS(if different from Controlling Office)	15. SECURITY CLASS. (of this report) UNCLASSIFIED
	15a. DECLASSIFICATION/DOWNGRADING SCHEDULE

16. DISTRIBUTION STATEMENT (of this Report)

Approved for public release; distribution unlimited.

17. DISTRIBUTION STATEMENT (of the abstract entered in Block 20, if different from Report)

18. SUPPLEMENTARY NOTES

19. KEY WORDS (Continue on reverse side if necessary and identify by block number)

DEFLAGRATION TO DETONATION TRANSITION
DDT
ROCKET COMBUSTION
SOLID ROCKET PROPELLANT
DETONATION
HMX
NITRAMINE PROPELLANT

20. ABSTRACT (Continue on reverse side if necessary and identify by block number)

Theoretical and experimental studies were undertaken to explain the mechanisms that establish conditions for the occurrence of the one-dimensional deflagration-to-detonation transition (DDT), and to formulate a satisfactory model for a quantitative description of this transiton. The theoretical studies were concerned with the thermo-hydrodynamic treatment of DDT. The central problem is to model the propagation of the unsteady flame and the flow it produces ahead of the flame front. The compressive flows produced by an accelerating flame and by an accelerating piston were compared to provide a better physical understanding of the compressive

DD FORM 1 JAN 73 1473

UNCLASSIFIED

SECURITY CLASSIFICATION OF THIS PAGE (When Data Entered)

action of an accelerating flame; conditions for shock formation in a compressive flow were formulated. The condition for shock formation in the compressed state is that the second derivative of the Lagrange pressure-specific volume compression curve be positive. When this condition is satisfied, a shock is always formed by an accelerating piston but not always by an accelerating flame. As the piston accelerates, the compression waves emanating from it overtake each other and coalesce to form a shock. But the accelerating flame can overtake and consume compressed material before the compression waves emanating from it coalesce to form a shock. In the experimental study, an assembly was designed to allow incorporation of stress gages into propellant charges during the casting process, thereby eliminating the expensive machining and grooving operations conventionally used in constructing targets for Lagrange gage experiments. Experimental procedures were developed for using multiple Lagrange stress gages to quantify states produced ahead of the flame front in burning HMX propellant. Internal pressure histories in compressed propellant were recorded for the first time in a DDT experiment. The gages recorded time periods of 300-500 μsec and peak pressures in the 2.5 to 4 kbar region. The limited pressure buildup is attributed to the small percentage of HMX in the propellant. A shock was not formed ahead of the flame because the second derivative of the Lagrange pressure-specific volume compression curve is negative in this pressure region.